

William R. Provancher
Mark R. Cutkosky

Dexterous Manipulation Lab
Stanford University, Stanford, CA, USA
wil@cdr.stanford.edu

Katherine J. Kuchenbecker
Günter Niemeyer

Telerobotics Lab
Stanford University, Stanford, CA, USA

Contact Location Display for Haptic Perception of Curvature and Object Motion

Abstract

We present a new tactile display for use in dexterous telemanipulation and virtual reality. Our system renders the location of the contact centroid moving on the user's fingertip. Constructed in a thimble-sized package and mounted on a haptic force-feedback device, it provides the user with concurrent feedback of contact location and interaction forces. We believe such a design will enable more versatile object manipulation and richer haptic interactions. To evaluate this display concept, we conducted two perceptual experiments. First, human subjects judged object curvature using both direct manipulation of physical models and virtual manipulation via the device. Results show similar levels of discrimination in real and virtual interactions, indicating the device can effectively portray contact information. Secondly, we investigated virtual interactions with rolling and anchored objects and demonstrated that users are able to distinguish the interaction type using our device. These experiments give insight into the sensitivity of human perception and suggest that even a simple display of the contact centroid location may significantly enhance telerobotic or virtual grasping tasks.

KEY WORDS—tactile display, tactile feedback, contact location, encountered object, haptics, perception, curvature, haptic rendering

1. Introduction

In the middle of the night the telephone rings. You grope for your glasses and fumble for the light switch. Among all the types of sensory information available to you at that moment, none is more important than knowing where objects are touching your fingertips. Early in the study of dexterous

manipulation, Fearing (1988) demonstrated that contact information is equally indispensable for manipulating objects in a robotic hand. Without this knowledge, grasp errors accumulate rapidly and the robot drops or damages the object. Subsequently, many robotics researchers developed tactile array sensors, capable of measuring contact location, pressure distribution and local object geometry (Lee 2000).

In contrast, tactile devices for displaying contact information in virtual reality or teleoperation have proven far more challenging. High-fidelity rendering of the local shape and pressure distribution at each fingertip requires a dense array of actuators. The peak force, velocity, and displacement necessary from each element all but preclude packaging the system at the fingertips of a standard haptic display system. The tactile displays that have appeared in the literature are instead benchtop devices, with a small array of pins in a stationary frame, actuated in the direction normal to the skin via wires or tubes (Hasser and Weisenberger 1993; Kontarinis et al. 1995; Pawluk et al. 1998; Moy, Wagner, and Fearing 2000) or stretching the skin in shear using piezoelectric actuators (Hayward and Cruz-Hernandez 2000).

As an alternative, displaying only the location of the centroid of contact on each finger requires far less extensive actuation. Even when objects are handled rapidly, the contacts progress along the fingertips at only a few centimeters per second. A single contact element can be moved over the surface of the finger in the proximal/distal and lateral directions using just two actuators (Figure 1(a)). The experiments reported in this paper consider only the proximal/distal location of the contact centroid, displayed using a roller as the tactile element that translates along the user's fingerpad (Figure 1(b)).

Most current haptic display systems treat contact even more simply than we propose, as a point force applied to the user's fingertip via a thimble. Incorporating contact-centroid motion into such interactions requires only minor system changes but can improve the interaction significantly. Such

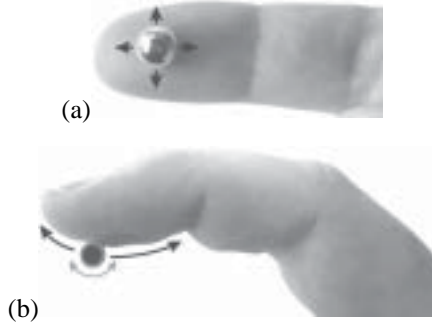


Fig. 1. Concept for contact location display. The (a) two-dimensional or (b) one-dimensional centroid of contact is represented with a single tactile element.

a display has the potential to simulate fingertip manipulation more realistically than traditional haptic devices, broadening the range of haptic interactions that can be rendered and experienced by users (see Provancher et al. 2003).

The idea of representing arbitrary contacts with a single moving element raises several interesting questions. Of primary concern is the manner by which people perceive differences in object curvature. Contact shape and pressure distribution both provide local object information (Srinivasan and LaMotte 1991). If this full set of tactile cues is not available, Montana (1988) suggests that the migration of the contact patch over the finger surface during manipulation can also be used to evaluate object curvature via rolling kinematics. This strategy for curvature perception is explored in the first experiment described herein. Contact location is also useful in other manipulation scenarios, such as rotating a scroll wheel or pushing a slider. In these cases, the migration of the contact patch can indicate rolling or sliding of the object relative to the finger, which is the subject of our second experiment.

To further explore these issues, we developed a device that can display contact location together with force feedback. Two separate experiments were conducted to evaluate the device and the user's relevant perceptions. The first study asked subjects to distinguish between objects of different curvature for both real and virtual interactions. The second experiment investigated the perceived motion of a virtual object, simulating rolling and anchored behaviors. The following sections describe the device, its control scheme, the two experiments, our conclusions, and the new research questions that this work raises.

2. Device Description

The contact location display system combines custom hardware with a standard haptic feedback device to render contact

location and force feedback simultaneously. Modulation of contact location is achieved through a one-degree-of-freedom linear mechanism attached to the user's forearm and finger, as shown in Figure 2(a). Placement of the linear mechanism on the forearm reduces device inertia at the hand and minimizes the transmission of actuator vibrations to the user's fingertip receptors. A series of interchangeable open-fingerpad thimbles was created using rapid-prototyping techniques (fused deposition modeling) to ensure a snug fit for subjects with a range of finger sizes.

As depicted in Figure 2(b), the contact element is attached to a desktop PHANToM, a commercial device commonly used for point-force feedback (Massie and Salisbury 1994). The PHANToM's encoders are used to measure the position of the user's finger in the vertical plane, and its motors provide reaction forces that are transmitted to the finger through the tactile element. An additional encoder measures the orientation of the thimble and finger in the vertical plane.

The tactile element is a small cylinder suspended beneath the user's fingertip. The cylinder can rotate freely or be prevented from rotating (using a small brake) to portray rolling or sliding contact, respectively. This contact element moves along the length of the thimble, about 2.0 cm, driven via two sheathed push-pull wires (0.61 mm diameter spring steel). A small DC motor actuates the wires via a leadscrew, continuously moving the roller to the appropriate location along the fingertip, as measured by the motor's encoder. The leadscrew in combination with the DC motor provided sufficient torque to overcome cable friction, which varied greatly with the user's hand and finger position. For more specific details about the design of the device, see Provancher (2003).

The tactile element is suspended underneath the fingertip by its two drive wires (nominal separation is 1–2 mm). In addition to their role in positioning the contact element along the length of the finger, the drive wires also act as a cantilever spring, effectively creating a series compliance between the haptic feedback device and the fingertip. The stiffness of this spring element is from 160 to 4300 N m⁻¹ depending on roller position. When the user's virtual finger is in free space, no forces are applied by the PHANToM and the cantilever stiffness of the drive wires prevents the contact element from touching the user's finger, leaving a gap as illustrated in Figure 3(a). When the user comes into contact with a virtual object, the system moves the tactile element to the correct location and applies a contact force. This force bends the drive wires and pushes the roller against the user's finger, as shown in Figure 3(b). Such an arrangement creates a realistic sensation of making and breaking contact by stimulating appropriate mechanoreceptors in the user's fingertip (Yoshikawa and Nagura 1999; Springer and Ferrier 2002). The simple addition of a linear positioning element and an open-bottom thimble transforms a standard haptic interface into a combined force and contact location display capable of portraying new kinds of interactions.

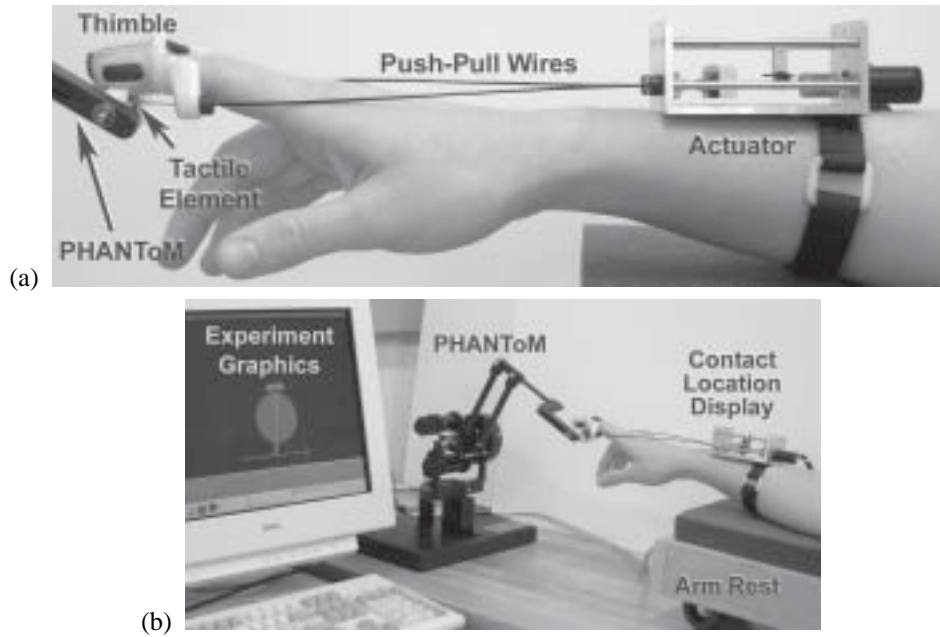


Fig. 2. (a) Contact location display system. Contact is rendered by a tactile element suspended beneath an open-bottom thimble. The tactile element is attached to a commercial haptic device to provide reaction forces to the finger. A small servo-motor provides precise positioning of the tactile element along the user's fingerpad via push-pull wires. (b) Experimental setup and graphics showing contact between the user's finger and a virtual object.

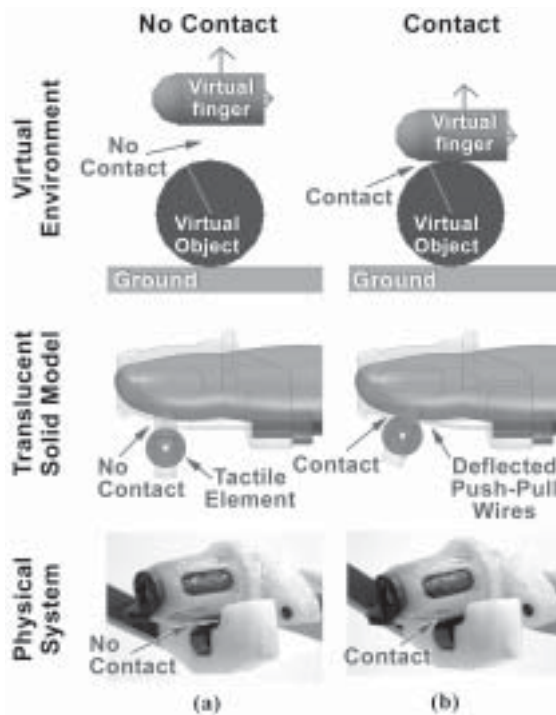


Fig. 3. (a) Free-space motion creates no contact with the tactile element. (b) Touching a virtual object yields contact.

3. Interaction model

Driving a device to display both contact location and force feedback requires a unique virtual interaction model. The system must treat the user's finger as an object, rather than a point, so that it can touch the environment at any location along its length. The position of contact along the finger must be continuously updated based on the user's motions and the geometry of the virtual environment. The tactile element must be positioned correctly both while in contact with an object and when in free space, in order to adequately anticipate future contacts. In this sense, the system is reminiscent of the "encountered object" class of haptic displays (Yokokohji et al. 2004). The algorithm that drives this continuous adjustment of contact location is based on simple geometric models of the user's finger and the environment.

For the experiments reported herein, the user's finger is modeled as a line segment, corresponding to the surface of the distal fingerpad. It has a segment length of 2.0 cm, equal to the length of travel of the contact display. The finger's configuration is described by \vec{x}_f , the position of its proximal endpoint, and ϕ , its angle from horizontal. Although the body of the finger is depicted in illustrations and on-screen graphics, the system does not consider the top, front, or back of the finger for collision detection. The virtual finger can touch the environment along its length or at either of the endpoints of the line segment (see Figure 4).

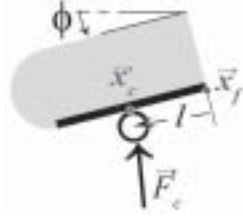


Fig. 4. The geometry of the finger model allows the controller to determine \vec{x}_f from the sensed parameters.

The interaction model for contact location display monitors the position of the user’s finger and also keeps track of a matching virtual finger. Following standard haptic display methods, this virtual finger acts as the user’s proxy in the virtual environment (Zilles and Salisbury 1995). It tracks the real finger’s motions in free space but remains on the surface of the environment during contact, minimizing separation to produce the desired position for the user’s finger, \vec{x}_{fd} .

As the user moves his or her finger up, down, forward and backward in the plane, the interaction model must determine the contact force, \vec{F}_c , and contact location, l , to display. Noting that the contact location display system cannot resist changes in finger angle, this variable is treated as a driven coordinate. The system calculates contact force based on the position difference between the real and virtual fingers. The user feels a force pushing his or her finger towards the location of the virtual proxy on the environment’s surface. While the user is touching the environment, the virtual finger’s contact location drives the tactile display, providing l_d , the desired position for the contact element. In the event of multiple contact points, the system renders the centroid of contact along the line segment. When the user’s finger is in free space, the device anticipates and tracks the closest point of contact so that the tactile element will be correctly positioned when the user touches the environment.

4. Controller

The system’s controller coordinates the hardware with the virtual world, as illustrated in Figure 5. The hardware is connected to a computer running RTAI Linux, which performs a real-time servo loop at 1 kHz. During each cycle, the controller samples the device’s encoders and computes the present finger position, finger orientation, and contact location using forward kinematics and the geometry shown in Figure 4. After the interaction model has processed the new configuration, control loops are closed around the desired positions for the finger and the contact element, and appropriate motor currents are commanded.

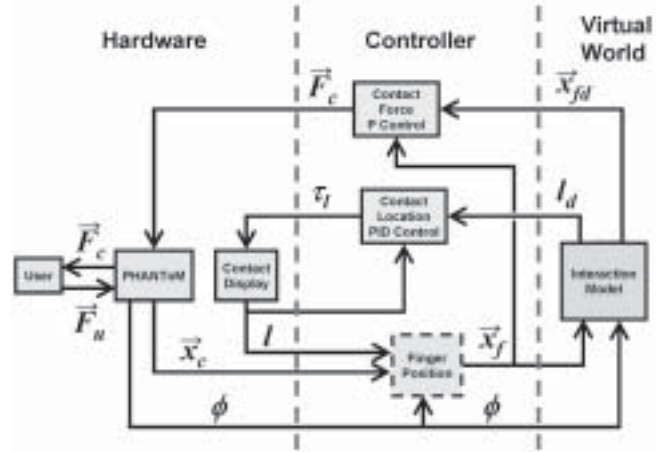


Fig. 5. System diagram. The controller connects the hardware to the virtual world, computing finger position, contact force, and contact location.

Table 1. System Diagram Nomenclature

Parameter	Description
\vec{x}_c	PHANToM endpoint position
l	contact location
ϕ	finger orientation
\vec{x}_f	finger position
\vec{x}_{fd}	desired finger position
l_d	desired contact location
\vec{F}_u	force applied by user
\vec{F}_c	contact force
τ_l	contact location positioning torque

4.1. Contact Force

Contact forces stem from differences between the user’s finger position, \vec{x}_f , and that of the virtual finger, \vec{x}_{fd} . The present interaction model simulates a simple stiffness, K_e , generating forces that are normal to the environment’s surface as follows:

$$\vec{F}_c = K_e(\vec{x}_{fd} - \vec{x}_f). \tag{1}$$

This contact force is rendered using the shoulder and elbow motors of the PHANToM, and it acts on the user through the tactile element. At maximum current, the device can output about 1.5 N in any direction, which easily deflects the drive wires and pushes the contact cylinder into the user’s fingertip. Future work on the interaction model could include simulated friction or other haptic cues in addition to stiffness.

4.2. Contact Location

The system uses a position control loop on the contact display's linear degree of freedom to track the interaction model's specified contact location, l_d . Proportional and integral forces draw the tactile element to its desired location along the fingertip. Local derivative feedback is used to damp out the dynamic oscillations excited by the push-pull wires and the stiction of the leadscrew. The entire contact location control law is

$$\ddot{F}_l = (K_p + \frac{K_i}{s})(l_d - l) - K_d s l, \quad (2)$$

where s is the Laplace operator. Because the leadscrew is non-backdrivable, the controller can force the tactile element to track its desired trajectory closely regardless of finger movements. The small-motion bandwidth of the roller is approximately 8 Hz for a travel of 1.0 cm. Roller positions along the finger are rendered with a maximum error of 0.05 mm for fast hand motions (5 cm s^{-1}) and an error of about 0.01 mm for the slow motions typically used by subjects. This simple PID controller yields good performance and stable operation for the contact location display hardware, enabling exploration of planar haptic environments.

5. Psychophysical Experiments

As expressed in the introduction, the idea of representing arbitrary contacts with a single moving element raises the question of how people perceive differences in object curvature. We conducted a series of human subject experiments to answer this question and understand how people will perceive the motion of virtual objects rendered via contact location feedback.

For the experiments described herein, the planar environment was always composed of a single circular object, and subjects interacted with only the top of this object. Furthermore, we constrained the virtual finger to remain horizontal, keeping $\phi = 0$. Motivated by hardware limitations, this choice simplified collision detection computations between the environment and the line segment representing the fingerpad. Later versions of the device include an encoder to measure the finger orientation as mentioned in Section 2. For treatment of the more general case with arbitrary object shapes, a curved fingerpad representation, and sensed finger orientation, see Kuchenbecker et al. (2004). Furthermore, to mimic the horizontal orientation of the virtual finger during the experiments, subjects were instructed to keep their finger horizontal and to make fore-aft motions with their arm as a whole. The rolling arm rest, shown in Figure 2(b), assisted in reinforcing these arm motions and improved user comfort. During experiments, subjects received interaction forces from virtual objects only in the vertical direction; however, they were also haptically guided to virtual objects during blindfolded testing by horizontal forces. Experiments on the discrimination of curvature and object motion are presented in the following subsections.

5.1. Curvature Discrimination for Real and Virtual Objects

A series of experiments was performed to quantify a user's ability to discriminate between objects of varying curvature. To simplify testing, only planar objects were studied, and the interaction was limited to horizontal motion of a single finger. This simplification allowed a comparison of results from direct physical manipulation and manipulation with virtual objects via the contact location display device. The experiments were designed following standard psychophysical procedures involving constant stimuli, with forced-choice comparisons between pairs of cases (Gescheider 1997). A description of the experimental protocol is given in Appendix A.

5.1.1. Experimental Setup and Procedure

These discrimination tests focused on the user's perception of curvature while rotating planar objects with a single finger. As illustrated in Figure 6(a), such a simple interaction is representative of more general object manipulation. In these tests, an explored object, whether real or virtual, pivoted about a fixed axis distinct from its center of curvature. This pivoting motion allowed the user to explore the curved surface using only a fingertip movement, feeling the contact travel along the distal fingerpad accordingly. This setup follows from the strategy of Montana (1988) for determining curvature when only information about the migration of contact position is available (i.e., no pressure distribution information), as is the case for virtual curvature discrimination tasks. The kinematics of this apparatus can be expressed as follows. Referring to Figure 7, we can derive an expression for the positions of the stimulus and the virtual finger based on the incremental finger movement Δx_f . For a given incremental finger movement Δx_f , a known rotation of the wheel, $\Delta\theta$, occurs that can be solved from the equation

$$\Delta x_f = R_d [\sin \theta_1 (1 - \cos \Delta\theta) - \cos \theta_1 \sin \Delta\theta] - r_c \Delta\theta, \quad (3)$$

where R_d is the distance between the pivot and the stimulus center of curvature, and θ_1 is the initial orientation of the stimulus. The stimulus rotation, $\Delta\theta$, can be solved from this non-linear equation by an appropriate method (e.g., Newton's method). Then the location of the point of contact with the stimulus, $\vec{x}_{stimulus} = [x_{stimulus} \ y_{stimulus}]^T$, can be expressed as follows:

$$x_{stimulus} = -R_d \sin(\theta_1 + \Delta\theta) \quad (4)$$

$$y_{stimulus} = R_d \cos(\theta_1 + \Delta\theta) + r_c. \quad (5)$$

These kinematics were programmed to drive the system's virtual interaction model, allowing appropriate variation of r_c and R_d . Correspondingly, real stimulus elements were manufactured for comparison; 14 test curves were arranged onto a

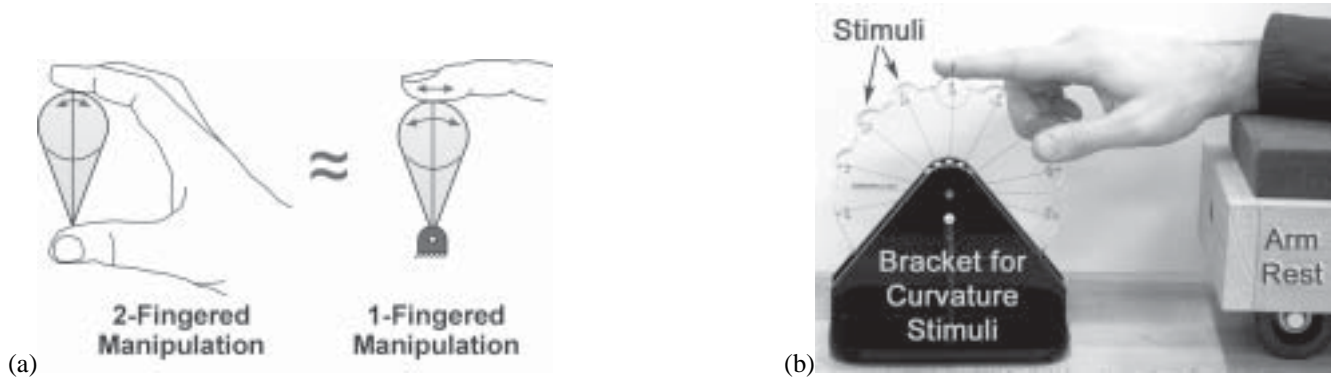


Fig. 6. (a) One-fingered planar perception of curvature provides a simplified form of object manipulation and highlights the use of contact location while exploring an object’s geometry. (b) The experiments were performed exploring 15° sectors of a “curvature wheel” for the direct manipulation. An arm rest helped users maintain horizontal motion.

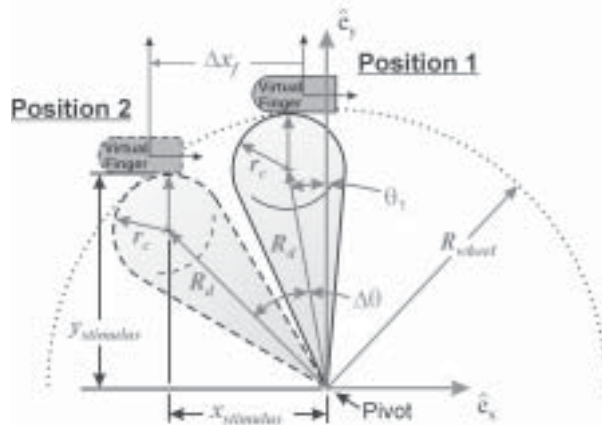


Fig. 7. Kinematics of virtual curvature apparatus. A simple kinematic model determines the current position of contact with the stimulus, $x_{stimulus}$ and $y_{stimulus}$, as a function of horizontal finger motion, Δx_f .

single “curvature wheel”, as shown in Figure 6(b). For each curve, the wheel could pivot 15°, corresponding to approximately ±1 cm of fingertip movement. The radius of curvature of the samples varied from 8.3 to 52.6 mm, centered around radius standards of 10, 20, 30, and 40 mm.

The curvature discriminations were conducted as a randomized series of comparisons in which users explored two stimuli and reported which of the two samples had a larger radius of curvature. For each comparison, one of the two samples was a standard value while the other was selected from among six smaller and larger neighboring sizes. The sizes were chosen to determine the just noticeable difference (JND; Gescheider 1997) relative to the standard size.

During the tests, subjects were blindfolded and used an armrest to maintain a horizontal finger orientation. Both real and virtual versions of the curvature wheel were presented in the same fashion. For the physical wheel, the limits of travel for each sector were indicated with spring-loaded ball detents; analogous force detents were implemented in software for the virtual wheel.

5.1.2. Results and Discussion

Figure 8 shows typical results for direct and virtual curvature comparison tests. These graphs represent the pooled responses of all subjects for the 40 mm standards. They plot the proportion of times subjects reported each stimulus as the larger of the two presented. As expected, the data have a sigmoidal distribution; stimuli that are considerably different from the standard are almost always correctly identified, while smaller differences are harder to discern. By convention, the JND for each standard is established as the average of the upper and lower difference thresholds (JND^U and JND^L ; see Figure 8), being the difference between 0.75 and 0.50, and 0.50 and 0.25 proportions respectively (Gescheider 1997).

Results for the other tested standards are similar and are summarized in Table 2. The data are shown as both the JND and the Weber fraction, where the Weber fraction is the ratio of the JND to the nominal stimulus value. The JNDs are also plotted against the nominal values in Figure 9. The direct discrimination data are slightly non-linear and are fit by a power curve (as suggested by Stevens’ power law; Gescheider 1997). In contrast, the virtual discrimination data are nearly linear with object size, in agreement with the underlying motion kinematics of the simulation. The average Weber fraction for virtual discriminations across the range of stimuli tested is 0.11.

Direct exploration of objects smaller than 25 mm in radius yields better performance (smaller JND) than virtual

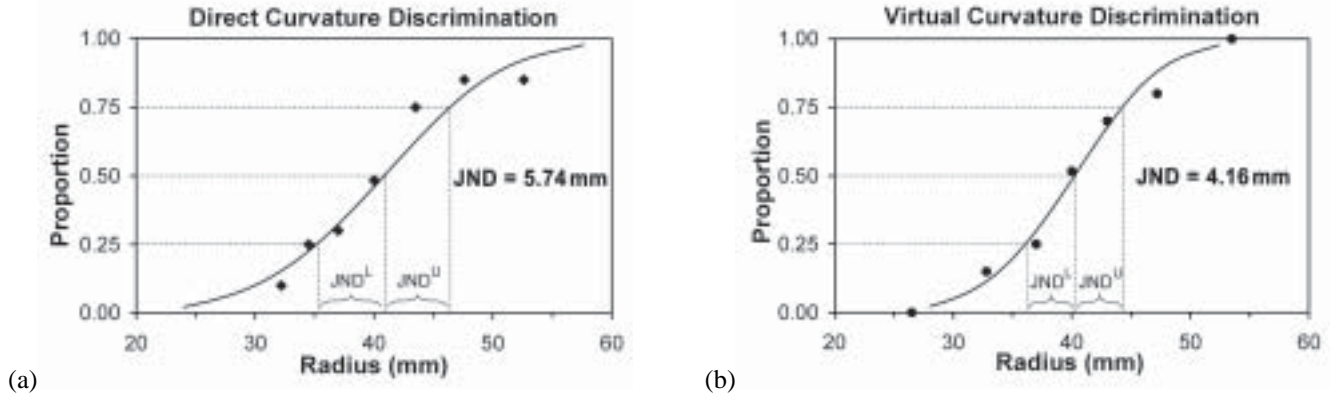


Fig. 8. Pooled results from all subjects for radius of curvature discriminations on the 40 mm standard during (a) direct physical interaction and (b) simulated virtual interaction rendered via the contact location display. The graphs display the proportion of times a particular stimulus was reported as having a greater radius of curvature. The JNDs are indicated with dotted lines.

Table 2. Results of Direct and Virtual Radius of Curvature Perception Experiments in the Form of JNDs and Weber Fractions for Each Curvature Standard

Nominal Radius (mm)	Direct Discrimination		Virtual Discrimination	
	Radius JND (mm)	Weber Fraction	Radius JND (mm)	Weber Fraction
10	0.84	0.084	1.35	0.135
20	1.49	0.074	2.25*	0.112*
30	4.00	0.133	3.77	0.126
40	5.74	0.143	4.16	0.104

*Data reported from pilot study representing five subjects.

discrimination. For small objects, local pressure distribution becomes the dominant mode of perception, which is not rendered by the virtual display. For radii above 30 mm, subjects performed better with virtual contacts. Here we believe the relatively small size of the roller in the contact display provides better localization and hence better contact movement cues than the larger contact patch experienced in direct manipulation. Subjects also commented that they found the larger radius virtual discriminations easier to perform than corresponding direct discriminations.

Following standard protocol, the anticipated factors that could impact experimental results were balanced. For example, half of the subjects completed direct curvature discrimination trials at the beginning of the experiment while the others began with virtual cases. Also, each of the combinations of stimuli was presented twice, with the order of presentation reversed the second time the trial was presented.

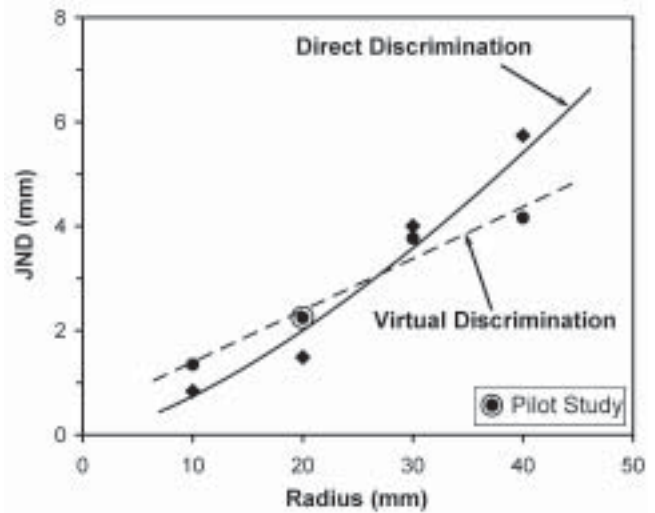


Fig. 9. JNDs of direct and virtual radius of curvature discrimination tests plotted versus their nominal stimuli value.

While balancing these effects is important for establishing perceptual thresholds, it is also informative to examine the data partitioned by these distinctions. An examination of these groups can reveal effects of learning and fatigue present in the experiment.

Statistical analysis of subjects' results partitioned into groups based on order of completion revealed two main findings. First, it was found that, in general, subjects performed better at the beginning of the experiment (by as much as 28%). This trend indicates that fatigue may have been a factor in the experiment. The second finding was that subjects were more

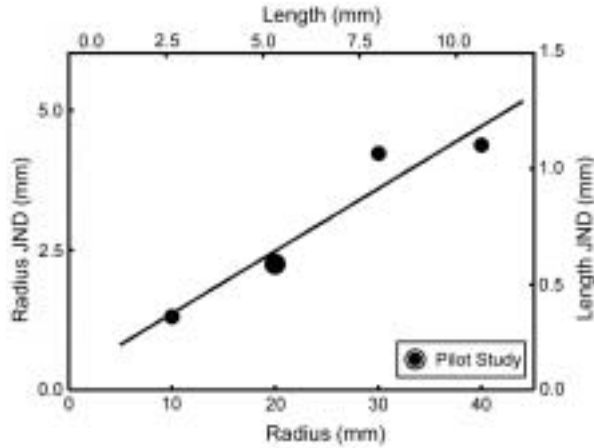


Fig. 10. JNDs for virtual radius of curvature discrimination tests reported as both radius- and length-based JNDs.

likely to make errors when the smaller of the pair of stimuli was presented first. For direct curvature discrimination, this was 30% more likely to occur; for virtual experiments 24% more likely. Presentation-order bias similar to that found in our experiments is quite common in psychophysical testing (Gescheider 1997).

By design, the contact location display relies on perception of motion on the fingertip. Limited to 15° sectors, objects with radii of curvature of 10, 20, 30, and 40 mm lead to nominal contact movements of 2.67, 5.33, 8.00, and 10.67 mm and JNDs of 0.36, 0.60, 1.01, and 1.11 mm, respectively. The results of virtual curvature discrimination experiments are replotted with both radius and length axes and corresponding JNDs in Figure 10. As with radius, the Weber fraction for tactile length discrimination averages to 0.11. This is consistent with the 10% Weber fraction reported by Biggs and Srinivasan (2002) for other length discriminations.

Many researchers have investigated the perception of curvature (Gordon and Morison 1982; Goodwin, John, and Marceglia 1991; Kappers, Koenderink, and Lichtenegger 1994; Louw, Kappers, and Koenderink 2002). The findings of Gordon and Morison (1982) and Goodwin, John, and Marceglia (1991) are especially relevant. Similar to the present experiments, each subject in these studies judged object curvature with the tip of the index finger. Figure 11 compares our curvature discrimination results to data presented by these researchers. Gordon and Morison (1982) had subjects actively explore plano-convex lenses with their fingertips. In contrast, Goodwin, John, and Marceglia (1991) pressed hemispherical stimuli onto the fingertips of their test subjects. These two experiments represent active and passive discrimination of curvature, respectively. As reported by Loomis and Lederman (1986), one would expect discriminations by active

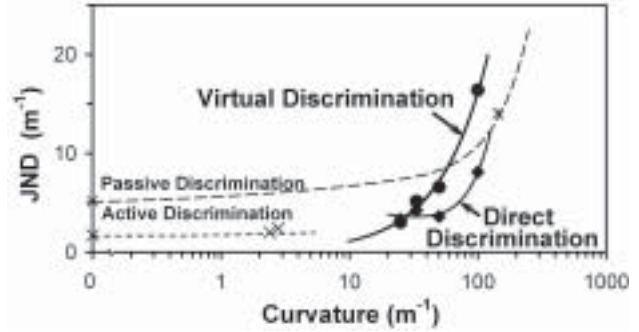


Fig. 11. Our results are framed by data reported in the literature for active fingertip curvature discrimination (Gordon and Morison 1982) and passive discrimination (Goodwin, John, and Marceglia 1991).

touch to be more accurate than those made by passive touch. While the current experiment has aspects of active touch, the motions of a subject's finger were somewhat restricted. Therefore, our results are expected to be bounded by those reported by Gordon and Morison (1982) and Goodwin, John, and Marceglia (1991). The data reported by Gordon and Morison represent the expected lower bound for the experiment, while perception of curvature via passive touch, reported by Goodwin, John, and Marceglia, represents the expected upper bound for the results. One can see that with the exception of extreme virtual cases, our data are indeed bounded.

While trends in the JND data hint at different perception strategies, especially at extreme object sizes, the magnitudes of the JNDs are similar for real and virtual tests. This experiment not only quantifies the user's perception capability but also validates the device's ability to effectively communicate information necessary for virtual object discrimination.

5.2. Perception of Virtual Object Motion

A second series of experiments was performed to investigate the user's perception of object motion via the contact location display. Relative movement of a grasped object provides important cues about the object's behavior and state. A simple test illustrates the applicability of our device for manipulation and sets the stage for its future use in robotic and haptic grasp control.

5.2.1. Experimental Setup and Procedure

Motion of an object can be described as anchored, rolling, or sliding, as shown in Figure 12. Changes in contact location along the fingerpad indicate relative movement between the finger and the object. At one extreme, sliding an object along a surface maintains a constant contact location on the fingertip.

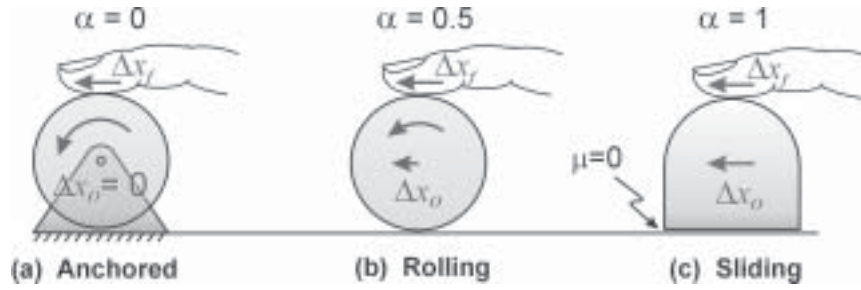


Fig. 12. Differences in apparent object motion can be described in terms of a ratio, $\alpha = \Delta x_o / \Delta x_f$, where Δx_o is the object displacement and Δx_f is the fingertip displacement. Values of α for familiar object motions are depicted above.

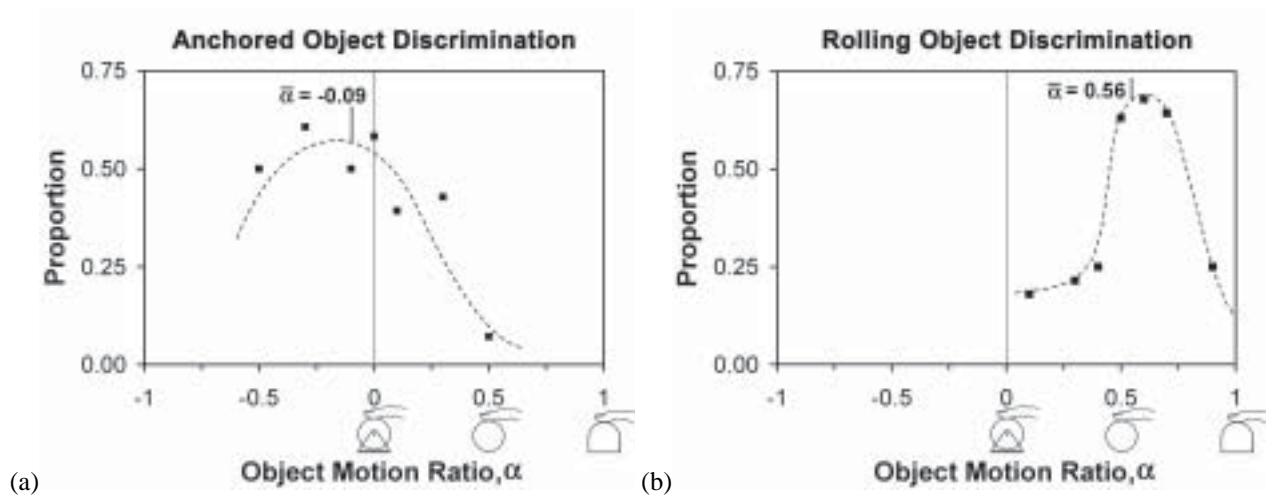


Fig. 13. The graphs display the proportion of times a given object motion ratio was reported as being (a) anchored or (b) rolling. The means of the anchored and rolling object distributions are -0.09 and 0.56 , respectively.

In contrast, rotating an anchored object fixes the contact in space regardless of finger motion. More generally, the object motion ratio, α , relates finger and object movements according to

$$\Delta x_o = \alpha \cdot \Delta x_f, \quad (6)$$

where Δx_f is the motion of the user's finger while in contact with the virtual object and Δx_o is the resulting object motion. These kinematics were programmed as a virtual environment, allowing for a range of α values.

Similar to the previous experiments, subjects were presented with a series of comparisons in which various object motion behaviors were presented. Ratios of $\alpha = -0.5 \dots 0.5$ were tested against a nominal anchored object with $\alpha = 0$ (Figure 12(a)). In a second series, ratios of $\alpha = 0.1 \dots 0.9$ were compared to a nominal rolling object with $\alpha = 0.5$ (Figure 12(b)). In each standard-based comparison, subjects

were asked which of the pair felt more anchored or rolling, respectively. The case of pure sliding (Figure 12(c)), with no motion relative to the fingertip, was not tested as it was too easy to distinguish from the other cases.

5.2.2. Results and Discussion

Figures 13(a) and (b) show the proportions of times that subjects identified a virtual object with a given value of α as anchored or freely rolling, respectively.

The means of the anchored and rolling distributions are -0.09 and 0.56 , respectively, falling close to their nominal values of 0.00 and 0.50 . This mismatch is an interesting perceptual result of these unsighted object manipulations, although its exact origin is unknown. Particularly noteworthy is users' preference for negative ratios in the anchored object tests. Unlike real objects, these objects move in opposition to the fingertip input, exaggerating normal sensations.

We believe that people evaluated object motion based on a comparison between absolute finger movement, observed kinesthetically, and relative contact centroid movement, observed cutaneously. Based on the results of our curvature discrimination experiment, we know that the cutaneous contribution to this comparison is quite accurate. Kinesthetic distance estimates are not nearly as reliable, which could explain the spread of the data. The standard deviation for rolling object tests was substantially smaller than for anchored objects, which we attribute to user experience rolling and manipulating objects by hand.

Looking at general trends in subject data, one interesting observation can be made. Over each set of 12 anchored object trials, many subjects chose objects with more negative α values towards the end of the set of trials. Perhaps this trend stems from users' unfamiliarity with energetic environments, which are not encountered in everyday manipulation. Users identified objects that actively rolled in opposition to their hand motion as feeling most anchored. No such trend was observed for perception of rolling objects.

Since direct and virtual curvature discrimination experiments were always completed back-to-back, the object motion experiments were completed either in the first or last ten minutes of the 1.5 hour long test session. An objective data analysis was completed on the object motion data to look for effects such as learning and fatigue. Subject data were partitioned into groups completing the object motion experiments at the beginning versus those completing motion experiments at the end of each session. Trends for both rolling and anchored object data were examined using single-factor ANOVA (90% confidence level) looking at the mean of each subject's test trials, $\bar{\alpha}_i$. This analysis showed that the performance of subjects in rolling behavior discriminations was unaffected by when they were completed in the test session ($p = 0.297$). However, it was observed that subjects completing the motion experiments at the end of the test session were closer identifying truly anchored object behavior, $\bar{\alpha} = -0.032$ compared to $\bar{\alpha} = -0.16$ for those performing motion experiments at the beginning of the test session ($p = 0.0545$).

The data were also partitioned according to whether the rolling or anchored discriminations were made first within the motion discrimination portion of the session (regardless of whether the motion experiments were completed at the beginning of the 1.5 hour long session or at the end). Once again, the performance of subjects in rolling behavior discriminations was unaffected by whether they were preceded by anchored discriminations ($p = 0.981$). Subjects completing anchored object discriminations after rolling discriminations were closer to identifying truly anchored object behavior ($\bar{\alpha} = -0.048$ compared to $\bar{\alpha} = -0.153$); however, this trend was not statistically significant ($p = 0.1549$). None the less, it does appear that subjects rapidly learned to correctly interpret the anchored object motion cues provided by the contact location feedback.

We also investigated the possibility of presentation-order effects (e.g., standard stimulus presented before comparison stimulus or stimuli presented with sequentially increasing value of α); however, no order bias was found for object motion experiments. Beyond the successful discrimination, subjects also commented that the object motion experiment felt realistic. These findings suggest that contact location feedback forms a promising new approach to tactile display.

6. General Discussion and Conclusions

In this paper we have presented a novel device for displaying contact centroid location during haptic interactions. Unlike pin arrays, it is easily mounted on a traditional haptic display and integrated with force feedback.

The contact location display system extends the paradigm of standard force-based haptic rendering by providing local tactile information. With this approach, the finger is no longer modeled as a point, but rather as a curve or a line segment. The length of this element corresponds to the travel of the tactile element along the user's finger. In contrast to previous force-only haptic interactions, the addition of contact location necessitates anticipation of collision to pre-position the tactile element.

In controlled experiments we found that human subjects could easily use the device to determine the curvature of virtual objects. Moreover, the JND values obtained with the device were comparable to those obtained with physical specimens and direct finger contact. Different trends between virtual and direct contact illustrate slightly different perception modes and lead to increased virtual discrimination for large radii of curvature.

The virtual objects were discriminated with a Weber fraction of approximately 0.11, indicating that users can detect changes in object radius greater than 11%. Based on the motion of the contact point, this finding also implies a tactile length Weber fraction of 0.11.

We also found that users of our device could identify various types of object motion based on the contact location change, specifically discerning rolling and anchored objects. Anecdotally, subjects reported that they found the sensation of traveling contacts a convincing simulation and a welcome improvement over probing the virtual world with a stylus or thimble.

The contact location display is a valuable addition to force-feedback for virtual and remote environments. We are encouraged that this approach will enable users to determine object geometry and changes in contact configuration during dexterous manipulation. The success also suggests many additional developments. The addition of friction to the environment model will improve the realism of local fingertip exploration. Conversion to two degrees of freedom would enable display of lateral as well as proximal/distal contact motion. We currently

mount our device on a grounded robotic arm; however, the device could also be used in combination with an ungrounded force-feedback device, such as Immersion's CyberGrasp. Finally, we believe that the development of a multifingered contact location display system would be particularly useful for dexterous manipulation, allowing users to feel object geometry and changes in contact configuration.

Appendix: Protocol for Discrimination Experiments

All experiments employed the method of constant stimuli with a paired-comparison forced-choice protocol to evaluate perceptual thresholds (JNDs) and sensitivity. To investigate perceptual sensitivity over a broad range, the experiment was divided into blocks. In each block, subjects were presented with stimuli clustered around a nominal value, referred to as a standard stimulus. Each standard was accompanied by six comparison stimuli (three larger and three smaller, presented twice each). Subjects were presented with two stimuli in rapid succession (separated by 2–4 s) and asked to state which met the specified condition. Standard methods were employed to prevent presentation-order bias (i.e., trial order was randomized and balanced). To isolate the effects of learning and fatigue, half of the subjects completed virtual discrimination experiments first. Subjects were blindfolded and wore sound insulating headphones to reduce distractions and ambient noise.

Sighted and blindfolded training preceded each block of testing. Virtual simulations were accompanied by computer graphics to reinforce haptic cues during training. Positive feedback on discrimination accuracy was provided at the beginning of curvature discrimination experiments. However, it was not provided in motion discrimination experiments to prevent habituation.

All subjects completed the experiment using the index finger of their right hand. For consistency between virtual and direct discrimination experiments, subjects performed these tests with their fingers extended and horizontal. Kinematic modeling assumed the finger orientation was always horizontal. The subjects' fingers were placed at the center of each stimulus at the start of each test. They made a single sustained contact with each stimulus and were not allowed to slide on the stimulus surface while exploring the physical models.

No time restrictions were placed on subjects during testing. However, to minimize the time required of each subject, tests were completed by two test groups. A majority of subjects completed the test in under 1.5 h. There were 14 people in first test group, which consisted of ten males and four females ranging in age from 20 to 34. All subjects in this group were right-handed. There were ten people in the second group, which consisted of eight males and two females ranging in age from 20 to 38. Two of the males in the second

group were left-handed. The number of people completing virtual or direct experiments first was equally balanced (i.e., for the second group, one left-handed and three right-handed males, and one female subject completed the virtual experiments first). Subjects completed a short questionnaire at the conclusion of the experiments.

Acknowledgments

This work was supported by the National Science Foundation (NSF) under grant NSF/IIS-0099636 and under KJK's NSF Graduate Research Fellowship. Special thanks to Susan Lederman for providing guidance in setting up the psychophysical experiments and to Mandayam Srinivasan for help in reviewing preliminary results. Thanks also to Vanessa Chial for programming the experiment graphics.

References

- Biggs, J. and Srinivasan, M. A. 2002. Haptic interfaces. *Handbook of Virtual Environments*, K. Stanney, editor, Chapter 5, Lawrence Erlbaum, London, pp. 93–116.
- Fearing, R. S. 1988. Tactile Sensing, Perception and Shape Interpretation. Ph.D. Thesis, Department of Electrical Engineering, Stanford University.
- Gescheider, G. 1997. *Psychophysics: The Fundamentals*, Lawrence Erlbaum Associates, NJ.
- Goodwin, A., John, K., and Marceglia, A. 1991. Tactile discrimination of curvature by humans using only cutaneous information from the fingerpads. *Experimental Brain Research* 86:663–672.
- Gordon, I. and Morison, V. 1982. The haptic perception of curvature. *Perception and Psychophysics* 31:446–450.
- Hasser, C. and Weisenberger, J. 1993. Preliminary evaluation of a shape-memory-alloy tactile feedback display. *Proceedings of the ASME Winter Annual Meeting, Symposium on Haptic Interfaces for Virtual Environments and Teleoperator Systems*.
- Hayward, V. and Cruz-Hernandez, J. 2000. Tactile display device using distributed lateral skin stretch. *Symposium on Haptic Interfaces for Virtual Environment and Teleoperator Systems*, pp. 1309–1314.
- Kappers, A. M. L., Koenderink, J. J., and Lichtenegger, I. 1994. Haptic identification of curved surfaces. *Perception and Psychophysics* 56(1):53–61.
- Kontarinis, D., Son, J., Peine, W., and Howe, R. 1995. A tactile shape sensing and display system for teleoperated manipulation. *Proceedings of the IEEE International Conference on Robotics and Automation*, Nagoya, Japan, May, pp. 641–646.
- Kuchenbecker, K. J., Provancher, W. R., Niemeyer, G., and Cutkosky, M. R. 2004. Haptic display of contact location. *Proceedings of the IEEE Haptics Symposium*, pp. 40–47.

- Lee, M. 2000. Tactile sensing: new directions, new challenges. *International Journal of Robotics Research* 19:636–43.
- Loomis, J. M. and Lederman, S. 1986. Tactual perception. *Handbook of Perception and Human Performance, Volume 2: Cognitive Processes and Performance*, Chapter 31.
- Louw, S., Kappers, A. M. L., and Koenderink, J. J. 2002. Active haptic detection and discrimination of shape. *Perception and Psychophysics* 64(7):1108–1119.
- Massie, T. H. and Salisbury, J. K. 1994. The PHANToM haptic interface: a device for probing virtual objects. *Proceedings of the ASME Winter Annual Meeting, Symposium on Haptic Interfaces for Virtual Environment and Teleoperator Systems*, November.
- Montana, D. 1988. The kinematics of contact and grasp. *International Journal of Robotics Research* 7:17–32.
- Moy, G., Wagner, C., and Fearing, R. 2000. A compliant tactile display for teletaction. *Proceedings of the IEEE International Conference on Robotics and Automation*, San Francisco, CA, April 24–28, pp. 3409–3415.
- Pawluk, D., Buskirk, C. V., Killebrew, J., Hsiao, S., and Johnson, K. 1998. Control and pattern specification for a high density tactile array. *Proceedings of the ASME Dynamic Systems and Control Division, International Mechanical Engineering Congress and Exposition*, New York, pp. 97–102.
- Provancher, W. R. 2003. On Tactile Sensing and Display. Ph.D. Thesis, Department of Mechanical Engineering, Stanford University.
- Provancher, W. R., Kuchenbecker, K. J., Niemeyer, G., and Cutkosky, M. R. 2003. Perception of curvature and object motion via contact location feedback. *Proceedings of the International Symposium on Robotics Research*, October, pp. 40–47.
- Springer, S. and Ferrier, N. 2002. Design and control of a force-reflecting haptic interface for teleoperational grasping. *Journal of Mechanical Design* 124:277–283.
- Srinivasan, M. A. and LaMotte, R. H. 1991. Encoding of shape in the responses of cutaneous mechanoreceptors. *Information Processing in the Somatosensory System*, O. Franzen and J. Westman, editors, Wenner-Gren International Symposium Series, Macmillan, London.
- Yokokohji, Y., Muramori, N., Sato, Y., and Yoshikawa, T. 2004. De-signing an encounter-type haptic display for multiple fingertip contacts based on observation of human grasping behavior. *Proceedings of the 12th Haptic Symposium on Haptic Interfaces for Virtual Environment and Teleoperator Systems*, Chicago, IL, March 27–28, pp. 66–73.
- Yoshikawa, T. and Nagura, A. 1999. A three-dimensional touch/force display system for haptic interface. *Proceedings of the IEEE International Conference on Robotics and Automation*, Detroit, MI, pp. 2943–2951.
- Zilles, C. and Salisbury, J. 1995. A constraint based god-object method for haptic display. *Proceedings of the IEEE/RSJ International Conference on Intelligent Robots and Systems*, Pittsburgh, PA.